

# Kramers–Kronig, Bode, and the meaning of zero

John Bechhoefer<sup>a)</sup>

Department of Physics, Simon Fraser University, Burnaby, British Columbia, Canada V5A 1S6

(Received 22 February 2011; accepted 29 June 2011)

The implications of causality are captured by the Kramers–Kronig relations between the real and imaginary parts of a linear response function. In 1937, Bode derived a similar relation between the magnitude (response gain) and the phase. Although the Kramers–Kronig relations are an equality, the Bode’s relation is effectively an inequality. This difference is explained using elementary examples and is traced back to delays in the flow of information within the system formed by the physical object and the measurement apparatus. © 2011 American Association of Physics Teachers. [DOI: 10.1119/1.3614039]

## I. INTRODUCTION

The Kramers–Kronig relations,<sup>1,2</sup> which connect the frequency-dependent real and imaginary parts of a linear response function, have wide applications. Part of their popularity resides in the generality of the Kramers–Kronig relations: they derive from causality, the response must follow the excitation and not precede it, and linearity, the superposition of responses to different causes.<sup>3,4</sup>

The generality of the Kramers–Kronig relations has made them a valuable tool, especially when measurements are limited or theory unclear. For example, in particle physics during the 1950s, the Kramers–Kronig relations and associated sum rules were helpful for making sense of scattering data and were used in S-matrix theory to analyze such experiments.<sup>5</sup> In optics, Bode’s gain-phase version of the Kramers–Kronig relations has been widely used to analyze the measurements of optical properties of materials, especially in reflection. If the light source is incoherent, only the magnitude of the reflection coefficient (the optics version of the gain) can be measured. The Bode relation then determines the phase. Given the magnitude and the phase, the index of refraction and absorption can be inferred.<sup>6–8</sup>

Although the Kramers–Kronig relations are part of the standard lore taught to graduate physics students, the corresponding relation between the magnitude and the phase of a complex response function is less well known outside its applications to optics, even though it was derived by Bode in 1937<sup>9</sup> and popularized by him in an influential 1945 text.<sup>10</sup> Even less appreciated is that although the Kramers–Kronig relations are an equality, the Bode gain-phase relation is, in effect, an inequality: systems can have an “extra” phase shift in their response that is greater than that given by the Bode relations. This extra phase shift has been repeatedly rediscovered in various physics contexts<sup>3,11,12</sup> and is often commented on with surprise and explained in ways that are more complicated than they need to be.

For reasons to be made clear, the Bode relation has been more appreciated by engineers than by physicists. I draw on the engineering literature and derive and explain the Bode relation and give several examples, where it is satisfied as an inequality rather than as an equality. From these examples, we will gain a better understanding of the Bode relation and of its implications, and a better appreciation that the measurement reflects the dynamics of a physical system, and how excitations are made and how signals are received. Carefully choosing the inputs and outputs of a system can help to eliminate surprises.

## II. THE KRAMERS–KRONIG RELATIONS

The Kramers–Kronig relations connect the real and imaginary parts of a causal linear response function,  $G(t)$ . We interpret  $G(t)$  as a Green function (or impulse-response function), which describes the response of a system at time  $t$  after being excited by a delta function at time 0. Causality implies that  $G = 0$  for  $t < 0$ . Linearity implies that the measurement  $y(t)$  in response to an excitation  $u(t)$  is given by

$$y(t) = \int_{-\infty}^{\infty} G(t-t')u(t')dt', \quad (1)$$

which implies that  $y(\omega) = G(\omega)u(\omega)$ . In the language of engineers,  $y(t)$  is the system output, and  $u(t)$  is the system input. The expression for  $y(\omega)$  follows from Fourier transforming and applying the convolution theorem and uses an “overloading” notation where the same letter denotes a function in both its time- and frequency-domain representations.

We are particularly interested in the frequency-domain response function,

$$G(\omega) \equiv G'(\omega) + iG''(\omega) = \int_0^{\infty} G(t)e^{i\omega t}dt, \quad (2)$$

where  $G'$  and  $G''$  are the real and imaginary parts of the response function, respectively. The lower limit in the integral in Eq. (2) is 0, not  $-\infty$ , because  $G(t)$  vanishes for  $t < 0$ .

We can extend the Fourier transform into the complex  $\omega$  plane and consider the complex function  $G$  over the  $\omega$  plane. Because  $G(t)$  is causal, the integral in Eq. (2) converges for real  $\omega$  if  $G(t)$  vanishes fast enough at large  $t$ . If it does, then the integral will converge even faster for  $\omega$  in the upper-half of the complex  $\omega$ -plane,<sup>13</sup> and it can be shown that  $G(\omega)$  is analytic in the upper-half plane.<sup>4</sup> From these properties of  $G$ , it is straightforward to derive the Kramers–Kronig relations<sup>13–15</sup> (see the Appendix)

$$G'(\omega) = \frac{2}{\pi}P \int_0^{\infty} \frac{\omega'G''(\omega')}{\omega'^2 - \omega^2}d\omega', \quad (3a)$$

$$G''(\omega) = -\frac{2\omega}{\pi}P \int_0^{\infty} \frac{G'(\omega')}{\omega'^2 - \omega^2}d\omega'. \quad (3b)$$

$P$  denotes the *Cauchy principal value*,<sup>13</sup> which is defined by excluding from the integration domain an infinitesimal region, that is, symmetrically distributed about the singular point,  $\omega$  [see the Appendix and Eq. (6b)]. We see that knowing the frequency dependence of the real part of the response

function is equivalent to knowing its imaginary part, and vice versa. Mathematically, the Kramers–Kronig relations in Eq. (3) are closely related to Hilbert transforms.<sup>13</sup>

### III. THE BODE GAIN-PHASE RELATION

The Kramers–Kronig relations lead to an analogous connection between the amplitude and the phase. Assume that the response function  $G(\omega)$  obeys the Kramers–Kronig relations and that there are no values of  $\omega$  in the upper-half of the complex  $\omega$ -plane for which  $G(\omega) = 0$ . If both conditions are satisfied, we can apply the Kramers–Kronig to the logarithm of the response function.<sup>16</sup> We note that  $\ln G(\omega) = \ln |G(\omega)| + i\varphi(\omega)$ , where  $\varphi(\omega)$  is the phase of the complex number  $G(\omega)$  at (angular) frequency  $\omega$ . Then Eq. (3) gives

$$\varphi(\omega) = -\frac{2\omega}{\pi} P \int_0^\infty \frac{\ln |G(\omega')|}{\omega'^2 - \omega^2} d\omega'. \quad (4)$$

As Bode recognized, Eq. (4) becomes more intuitive after integrating by parts. First, we let  $\nu \equiv \ln(\omega'/\omega)$ , or  $\omega' = \omega e^\nu$ , and  $M(\nu) \equiv \ln |G(\omega')|$ , giving

$$\varphi(\omega) = -\frac{2}{\pi} P \int_{-\infty}^\infty \frac{\phi M(\nu)}{\phi^2 (e^{2\nu} - 1)} \phi e^\nu d\nu, \quad (5a)$$

$$= -\frac{1}{\pi} P \int_{-\infty}^\infty \frac{M(\nu)}{\sinh \nu} d\nu. \quad (5b)$$

Because the sinh function is odd, only the odd part of  $M(\nu)$  contributes in Eq. (5b). We write  $M$  as the sum of odd and even functions,  $M = M_o + M_e$  and have

$$P \int_{-\infty}^\infty \frac{M(\nu)}{\sinh \nu} d\nu = \lim_{\varepsilon \rightarrow 0^+} \left\{ \int_{-\infty}^{-\varepsilon} + \int_{\varepsilon}^\infty \right\} \left[ \frac{M_o(\nu) + M_e(\nu)}{\sinh \nu} \right] d\nu, \quad (6a)$$

$$= 2 \lim_{\varepsilon \rightarrow 0^+} \int_{\varepsilon}^\infty \frac{M_o(\nu)}{\sinh \nu} d\nu, \quad (6b)$$

because the even contributions  $M_e$  cancel in the two integrals. We next integrate by parts, noting that  $\int d\nu / \sinh \nu = -\ln \coth \nu/2$ . Hence Eq. (6b) becomes

$$2 \lim_{\varepsilon \rightarrow 0^+} \left\{ \int_{\varepsilon}^\infty \frac{dM_o}{d\nu} \ln \coth \frac{\nu}{2} d\nu - M_o \ln \coth \frac{\nu}{2} \Big|_{\varepsilon}^\infty \right\}. \quad (7)$$

As  $\nu \rightarrow \infty$ ,  $\ln \coth \nu/2 \sim 2e^{-\nu} = 2\omega/\omega'$ . As  $\omega' \rightarrow \infty$ ,  $|G(\omega')| \sim \omega'^{-n}$ , because the physical response functions vanish at infinite frequencies. Thus  $\ln |G| \sim -n \ln \omega'$ , and  $M_o(\nu) \ln \coth \nu/2 \sim \ln \omega'/\omega' \rightarrow 0$ .

As  $\nu \rightarrow 0$ ,  $\ln \coth \nu/2 \approx -\ln \nu/2$ . Because  $M_o$  is odd,  $M_o \sim \nu + \mathcal{O}(\nu^3)$ . We thus find  $\nu \ln \nu \rightarrow 0$ . Thus,

$$\varphi(\omega) = -\frac{2}{\pi} \int_0^\infty \frac{dM_o}{d\nu} \ln \coth \frac{\nu}{2} d\nu, \quad (8a)$$

$$= -\frac{1}{\pi} \int_{-\infty}^\infty \frac{dM}{d\nu} \ln \coth \frac{|\nu|}{2} d\nu, \quad (8b)$$

where in the last step, we used  $2M_o = M(\nu) - M(-\nu)$ .

Finally, we have Bode's gain-phase relation<sup>17,18</sup>

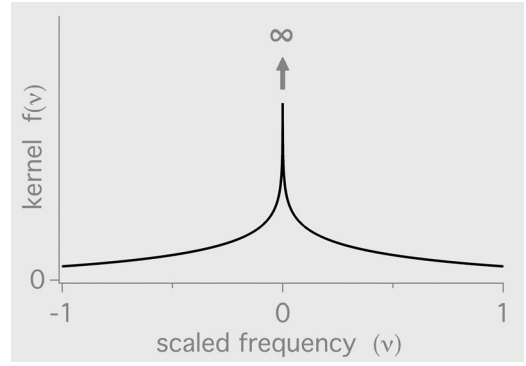


Fig. 1. Kernel  $f(\nu)$ , with scaled frequency  $\nu = \ln \omega'/\omega$ .

$$\varphi(\omega) = -\frac{\pi}{2} \int_{-\infty}^\infty \frac{dM}{d\nu} f(\nu) d\nu \quad (9a)$$

$$f(\nu) \equiv \frac{2}{\pi^2} \ln \coth \frac{|\nu|}{2}, \quad (9b)$$

where the kernel  $f(\nu)$  resembles a broadened delta function about  $\nu = 0$  (see Fig. 1), where  $\omega' = \omega$ . The kernel is normalized so that  $\int_{-\infty}^\infty f(\nu) d\nu = 1$ .

To understand the implications of the Bode relation, consider the frequency response  $G(\omega) \sim \omega^{-n}$ . Such a relation typically holds at high frequencies for the physical response functions. For example, a low-pass filter has  $n = 1$ , and a harmonic oscillator has  $n = 2$ . If this relation holds for all frequencies  $\omega > 0$ , then

$$\frac{dM}{d\nu} = \frac{d \ln |G|}{d \ln \omega} = -n, \quad (10)$$

and the phase delay is  $n\pi/2$ . More generally,  $n(\omega)$  is the local value of  $\ln |G(\omega)|$ . In that case, we note that the kernel  $f(\nu)$  in Fig. 1 resembles a broadened delta function, with most of its weight near  $\nu = 0$  ( $\omega' = \omega$ ). If  $n(\omega)$  is constant over about a decade of frequency centered on  $\omega$ , then the Bode relation is approximately

$$\varphi(\omega) \approx -\frac{\pi}{2} \frac{d \ln |G(\omega)|}{d \ln \omega} \approx \frac{\pi}{2} n(\omega). \quad (11)$$

As a result, when the frequency response is graphed on Bode plots with logarithmic frequency axes and a logarithmic magnitude axis, the phase lag is approximately the derivative of the magnitude curve times  $\pi/2$ .

### IV. BODE RELATION AND OPTICAL RESPONSE

In Sec. I, we noted that one of the important applications of the Bode gain-phase relation is the determination of the optical properties of materials. The method is especially useful in the far infrared, where there is a lack of bright, tunable, and coherent sources. Instead, we typically measure the reflectance  $R = |r|^2$  as a function of frequency  $\omega$ , where the reflection coefficient  $r$  is the complex linear response function  $r = E_{\text{ref}}/E_{\text{in}}$ , the ratio of reflected to incident electric fields. Because the source is incoherent, we cannot use the interference techniques that would normally help to determine the phase. Hence, only  $R(\omega)$  is typically available, and we must numerically integrate the Bode's gain-phase relation, Eq. (9) with  $R = G$  to determine the phase

$\varphi(\omega) = \arg R(\omega)$ . For a thick sample whose reflectance is measured at normal incidence, we then use the Fresnel relation to write<sup>8</sup>

$$r = \sqrt{R}e^{i\varphi} = \frac{n + ik - 1}{n + ik + 1}, \quad (12)$$

where  $n(\omega)$  is the index of refraction, and  $k(\omega)$  is the absorption coefficient. Given the complex  $r(\omega)$ , we solve for  $n$  and  $k$  numerically.

In practice, there are a number of issues, the most important of which is that the reflectance  $R(\omega)$  can be measured only over a limited frequency range, and it is necessary to make some plausible guesses to extrapolate  $R$  to all frequencies in the numerical integration of the Bode relation.<sup>11</sup> As long as we work with normal incidence and thick samples, the method makes possible highly accurate inferences of the phase and hence of the behavior of  $n$  and  $k$ . As we have mentioned, the technique is the standard one for such measurements in the far-infrared frequency range.

For oblique incidence or thin films, there are many cases where the phase that is deduced from the Bode relation underestimates the actual phase shift and hence leads to incorrect inferences for the material parameters.<sup>8,11</sup> The failure of a naive application of the Bode relation in this and other cases motivates a closer look at the underlying physics.

## V. NON-MINIMUM-PHASE RESPONSE FUNCTIONS

Bode's relation, Eq. (9), is an equality for response functions that are analytic in the upper-half plane (and thus obey the Kramers–Kronig relations) and, in addition, have no zeros in the upper-half plane. Yet many physical response functions that are causal and obey the Kramers–Kronig relations do have zeros in the upper-half plane. These response functions have extra phase delays: the phase lag at a given frequency is greater than that predicted by the Bode relation. Because these response functions are physical as we will see in several examples, it is reasonable to interpret the Bode relation as an inequality.

As an example, consider the response function for the delay  $\tau$ , with output  $y(t) = u(t-\tau)$ . The Fourier transform is

$$y(\omega) = e^{i\omega\tau}u(\omega), \quad (13)$$

and we can identify the response function of the delay as  $G_{\text{delay}} = e^{i\omega\tau}$ . Because  $G_{\text{delay}}(\omega)$  has an essential singularity at  $|\omega| \rightarrow \infty$ , the logarithm is not analytic at infinity, and the Bode relation does not apply. However, a delay is a physically possible, causal response function, and its real and imaginary components,  $G'(\omega) = \cos \omega\tau$  and  $G''(\omega) = \sin \omega\tau$ , satisfy the Kramers–Kronig relations, as may be verified by substitution into Eq. (3).

The magnitude and phase are  $|G_{\text{delay}}| = 1$  and  $\varphi_{\text{delay}} = \omega\tau$ . In contrast, if there is no delay, then  $G_{\text{delay}}(\tau = 0) \equiv G_0 = 1$ , which has  $|G_0| = 1$  but  $\varphi_0 = 0$ . Thus, we have two response functions, with equal magnitude response but different phase lags. Applying the Bode's relation to both response functions predicts zero phase lag for both. (The exponent  $n = 0$ .)

We have seen that if a response function contains a delay, the phase lag exceeds that predicted by the Bode relation. Because causality precludes a phase advance, we conclude that the Bode relation gives the minimum phase lag. Such minimum-phase response functions have the smallest phase

lag that is compatible with a given magnitude response. Non-minimum-phase response functions have a larger phase lag.

In addition to an exact delay, there are other non-minimum-phase response functions that act as approximate delays. Consider the family  $G_n(\omega)$  of  $n$ th-order rational (Padé) approximations to the unit delay  $G_{\text{delay}} = e^{i\omega}$ . The first- and second-order approximations are

$$G_1 = \frac{1 + \frac{1}{2}i\omega}{1 - \frac{1}{2}i\omega}, \quad G_2 = \frac{1 + \frac{1}{2}i\omega - \frac{1}{12}\omega^2}{1 - \frac{1}{2}i\omega - \frac{1}{12}\omega^2}, \quad (14)$$

The functions  $G_n$  all have unit magnitude. For example,

$$|G_1(\omega)| = \left[ \left( \frac{1 - \frac{1}{2}i\omega}{1 + \frac{1}{2}i\omega} \right) \left( \frac{1 + \frac{1}{2}i\omega}{1 - \frac{1}{2}i\omega} \right) \right]^{1/2} = 1. \quad (15)$$

Response functions such as these with unit magnitude response for all frequencies are known as *all-pass* functions. (Because of this property, a Padé expansion is more useful than a Taylor expansion.) We can easily verify that the high-frequency phase lag of  $G_n$  is  $n\pi/2$ . Figure 2(a) shows the Bode plots and Fig. 2(b) the time responses to a unit step for  $G_{\text{delay}}$ ,  $G_1$ , and  $G_2$ . We note that  $G_1$  and  $G_2$  approximate a delayed response, and the transients show an “inverse response” relative to the final value. The transient for  $G_n(t)$  crosses the zero axis  $n$  times before approaching its asymptotic value of one. The other feature of the Padé approximates is that  $G_1$  and  $G_2$  have zeros in the upper-half of the complex  $\omega$  plane, as is usual for non-minimum phase response functions, and poles in the mirror position of the lower half of the  $\omega$  plane [see Fig. 2(c)].

Although the all-pass functions we have considered might seem to be a special case of functions with zeros in the upper complex plane, an arbitrary non-minimum-phase response function can always be expressed as the product of a minimum-phase function and an all-pass function.<sup>19</sup> That is,

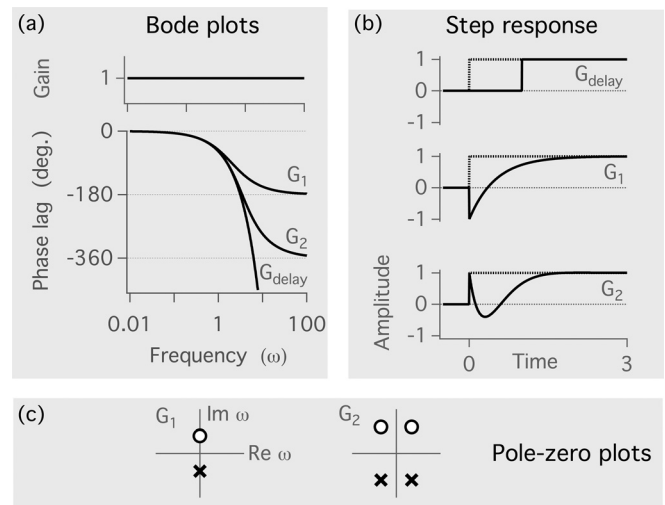


Fig. 2. All-pass approximations to a unit delay. (a) Bode plots of  $G_1$ ,  $G_2$ , and  $G_{\text{delay}}$ . (b) Responses to a unit step. (c) Pole-zero plots for  $G_1$  ( $z = 2i$ ,  $p = -2i$ ) and  $G_2$  ( $z = 3i \pm \sqrt{3}$ ,  $p = -3i \pm \sqrt{3}$ ). Zeros are denoted by  $\circ$ , poles by  $\times$ .

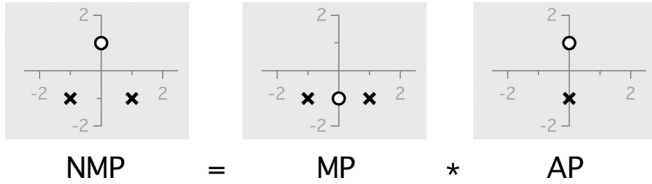


Fig. 3. Decomposition of the non-minimum phase  $G(\omega) = (1 + i\omega)/(-\omega^2 - 2i\omega + 2)$  into the product of a minimum-phase  $(1 - i\omega)/(-\omega^2 - 2i\omega + 2)$  and an all-pass response function  $(1 + i\omega)/(1 - i\omega)$ .

$$G(\omega) = G_{\text{MP}}(\omega)G_{\text{AP}}(\omega), \quad (16)$$

where  $G_{\text{MP}}$  is minimum phase and  $G_{\text{AP}}$  is all pass.

To see this result, note that either  $G(\omega)$  is either already minimum phase or has zeros at  $\omega = \{iz_1, iz_2, \dots\}$ . Let us define the *Blaschke product*<sup>3</sup>

$$G_{\text{AP}}(\omega) = \left( \frac{z_1 + i\omega}{z_1^* - i\omega} \right) \left( \frac{z_2 + i\omega}{z_2^* - i\omega} \right) + \dots, \quad (17)$$

which is all pass. Because  $G(t)$  is real, if there is a complex zero, its conjugate is also a zero, as seen for  $G_2(\omega)$  in Fig. 2(c).

We define  $G_{\text{MP}} = G/G_{\text{AP}}$ , which swaps the upper-plane zeros for their mirror reflection in the lower plane. For example,

$$\begin{aligned} G(\omega) &= \underbrace{\frac{1 + i\omega}{-\omega^2 - 2i\omega + 2}}_{\text{non-minimum phase}} \\ &= \underbrace{\left( \frac{1 - i\omega}{-\omega^2 - 2i\omega + 2} \right)}_{\text{minimum phase}} \underbrace{\left( \frac{1 + i\omega}{1 - i\omega} \right)}_{\text{all pass}}. \end{aligned} \quad (18)$$

Note in Fig. 3 how the zero of  $G(\omega)$  at  $\omega = i$  has been transferred to the all-pass function, and the minimum-phase function substitutes a reflected zero at  $\omega = -i$ . The poles at  $-i \pm 1$  are untouched.

## VI. EXAMPLES AND APPLICATIONS

We have seen that a response function has a phase lag that exceeds the amount predicted by the Bode's gain-phase theorem when there is a zero in the upper-half of the complex  $\omega$  plane. In this section, we present examples of systems that show such non-minimum-phase behavior.

### A. Flexible and multimode objects

One class of systems that are often non-minimum-phase are flexible objects—ones whose dynamics show contributions from many modes. Often, the modes are extremely underdamped. As a toy model of a flexible system, consider a system whose output adds contributions from two undamped modes, with frequencies scaled to 1 and  $\omega_0$ . If the mode amplitudes are  $\pm\alpha$  and  $\beta$ , the response in the frequency-domain is

$$G_{\pm}(\omega) = \pm \frac{\alpha}{1 - \omega^2} + \frac{\beta}{1 - \frac{\omega^2}{\omega_0^2}} \quad (19a)$$

$$= \frac{\pm\alpha + \beta - \left( \frac{\pm\alpha}{\omega_0^2} + \beta \right) \omega^2}{(1 - \omega^2) \left( 1 - \frac{\omega^2}{\omega_0^2} \right)}, \quad (19b)$$

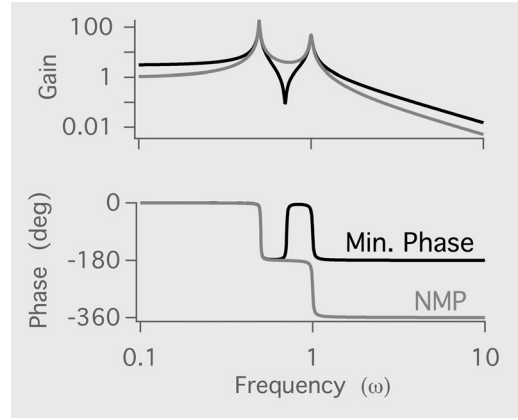


Fig. 4. Two-mode dynamics Bode plot from Eq. (19b), with  $\alpha = 1$ ,  $\beta = 2$ , and  $\omega_0 = 0.5$ . Black line: minimum-phase case,  $G_+$ . Gray line: non-minimum-phase case,  $G_-$ . A small amount of damping has been added to simplify the phase plots.

which implies that

$$z^2 = \frac{\pm\alpha + \beta}{\frac{\pm\alpha}{\omega_0^2} + \beta}. \quad (20)$$

Note how adding two oscillatory modes create two zeros (given by  $z$ ), whose locations depend on the mode amplitudes  $\alpha$  and  $\beta$ .

Figure 4 shows Bode plots for a case where  $\alpha$  and  $\beta$  are chosen so that  $G_+$  is minimum phase and  $G_-$  is non-minimum-phase. The minimum-phase function has an asymptotic phase lag of  $180^\circ$ , as expected for a system of relative order equal to 2, and that of the non-minimum-phase system is larger ( $360^\circ$ ). We have added a small amount of damping ( $\zeta = 0.01$  for each mode) to soften the phase jumps and to keep the responses finite. The damping shifts the poles and zeros slightly below the real axis in the complex  $\omega$ -plane. The poles then are strictly in the lower half of the  $\omega$  plane, as they must be for a stable system. With damping, the zeros give rise to finite-magnitude response minima, known as *antiresonances*.

Doyle *et al.*<sup>20</sup> have shown that this two-mode toy model has a simple realization (see Fig. 5). A horizontal mass supported by two springs undergoes an infinitesimal vertical displacement  $z(t)$  and rotation  $\theta(t)$ . If a force  $u(t)$  is applied at the distance  $\ell_u$  to the right of the center of mass, the equations of motion are

$$m\ddot{z} + kz = u, \quad (21a)$$

$$I\ddot{\theta} + k\ell^2\theta = \ell_u u, \quad (21b)$$

where  $m$  is the mass of the block,  $I$  its moment of inertia about the center of mass, and each spring has a spring constant  $\frac{1}{2}k$  (see Fig. 5). Now—and this is the important step—consider measuring the position of the block at one of the two places  $y_{\pm} = z \pm \ell_u\theta$ ;  $y_+(t)$ , is located where the force is applied, and  $y_-(t)$  is at the symmetric location,  $\ell_u$ , to the left of the center of mass. If we Fourier transform Eq. (21b) and calculate the response of  $y_{\pm}(\omega)$  to the input  $u(\omega)$ , we find a function of the form of Eq. (19b), where  $m = 2$ ,  $k = I = 1/2$ ,  $\ell = 1$ , and  $\ell_u = 1/\sqrt{2}$ , for the example, plotted in Fig. 4.

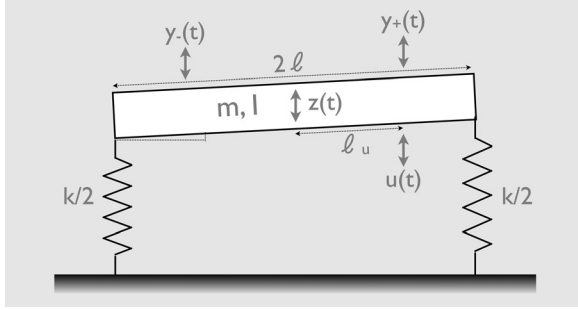


Fig. 5. Object of mass  $m$ , length  $2\ell$ , and moment of inertia (about the center of mass)  $I$  supported by two springs, each with force constant  $k/2$ . The vertical displacement from the center of mass is  $z$ . A force  $u(t)$  is applied at the right at position  $\ell_u$ . The force also acts as a torque. The output is the vertical displacement,  $y(x, t)$ , measured at a point  $x$  along the bar. At the right edge ( $x = \ell$ ), the measurement is denoted by  $y_+(t)$ ; at the left edge ( $x = -\ell$ ) it is denoted by  $y_-(t)$ .

Thus, if we measure the position of the block where the force is applied, the response is minimum-phase. If measured at the opposite side, the response is non-minimum-phase. In engineering jargon, the former case is a *collocated* measurement and the latter a *non-collocated* measurement.

The situation is similar, but more complicated, when considering a flexible object whose motion is the sum of many modes. Because each mode has a  $180^\circ$  phase shift, the alternating pattern of poles and zeros seen in Fig. 4 persists, with a zero between each resonance. If the system is minimum phase, the maximum phase shift continues to be  $180^\circ$ , no matter how many modes are relevant. Such ideas are important in the analysis of atomic force microscopes, which use a flexible cantilever to probe a surface. The speed at which a surface can be scanned is limited by the response of the cantilever to forces created by the variable surface topography. Certain combinations of inputs and outputs lead to minimum-phase response, while others lead to non-minimum-phase response.<sup>21</sup> A design without unnecessary non-minimum-phase zeros allows higher scan rates.

## B. Optical systems

Optical systems provide many examples of zeros (for example, destructive interference). Here, we give two examples where the response is non-minimum phase. The first, which we introduced in Sec. IV, occurs in the analysis of reflectance spectra, where the goal is to infer the complex phase shift as a function of light frequency from the measured reflectances. The generalization of the Fresnel relation, Eq. (13), to an oblique angle of incidence  $\theta$  gives, for TM radiation on a thick sample,

$$r_{\text{TM}}(\omega) = \frac{n^2 \cos \theta - \sqrt{n^2 - \sin^2 \theta}}{n^2 \cos \theta + \sqrt{n^2 - \sin^2 \theta}}, \quad (22)$$

where  $n(\omega)$  is the complex index of refraction of the material of interest (in air, for simplicity). As Peiponen and Saarinen discuss,<sup>8</sup> the response function  $r_{\text{TM}}(\omega)$  can have an upper-plane zero for complex  $\omega$  for some combinations of  $n$  and  $\theta$ . In such circumstances, there will be phase shifts beyond what the Bode relation predicts. If we do not take into account the extra phase shifts, the inferred absorption will be incorrect. The easiest fix is to choose conditions (for example, a thick sample at normal incidence) where the response

is minimum phase. Unfortunately, for a thin film, the zeros associated with Fabry–Perot resonances are typical at all angles.<sup>11</sup> If conditions leading to zeros cannot be avoided, independent measurements are needed to determine the phase. Measuring the reflectances at different angles is one possibility.

The second example occurred in a recent analysis of phase-sensitive measurements of microwaves propagating through a waveplate.<sup>12</sup> Although the focus of the work was to show that birefringence could lead to superluminal group velocities, it was also noted that the phase shift showed an abrupt increase when the analyzer polarization angle was rotated past  $45^\circ$  with respect to the optical axis of the waveplate. For example, a linearly polarized wave incident at  $45^\circ$  with respect to the optical axis and analyzed at an angle  $\beta$  has an electric field

$$E(\omega) \propto e^{i\phi_{\text{TM}}} [\sin \beta e^{i\Delta\phi} + \cos \beta], \quad (23)$$

where  $\Delta\phi(\omega) = \Delta n(\omega) \omega d/c$ , with  $d$  the thickness of the waveplate and  $c$  the speed of light. Here,  $\Delta n(\omega)$  is the frequency-dependent birefringence of the waveplate, and  $\phi_{\text{TM}}$  is the phase shift of the TM wave. In Eq. 24,  $E(\omega) = 0$  when, for integer  $m$ ,

$$\Delta\phi^* = -i \ln |\cot \beta| + 2\pi \left( m + \frac{1}{2} \right). \quad (24)$$

As  $\beta$  is varied about  $45^\circ$ ,  $\cot \beta$  is larger or smaller than 1, so that  $\text{Im } \Delta\phi^*$  is larger or smaller than 0. Because  $\Delta\phi \sim \omega \Delta n(\omega)$  and  $\Delta n$  is approximately real (and positive) for the conditions of the experiment, the zeros determined by  $\omega^* \propto \Delta\phi^*$  change from the lower to the upper-half plane for  $\beta > 45^\circ$ .<sup>22</sup>

## C. Implications for feedback control

Upper-plane zeros and non-minimum-phase response functions are more familiar in engineering than in physics. The reason is that the extra delays lead to problems when attempting to embed a non-minimum-phase system inside a feedback loop.<sup>23,24</sup> The basic ideas are simple: In a feedback loop, the goal is typically to regulate or track a reference signal. Any difference (or error) is used to generate a correction signal. But phase lags due to the time it takes signals to propagate from input to output can make the control have the wrong correction. In particular, if a sinusoidal signal lags by  $180^\circ$ , the correction will be exactly in the wrong direction (positive feedback). If the amplitude grows for each feedback loop, there will be a runaway oscillatory instability. Non-minimum-phase systems exacerbate this problem by adding to the phase lag. In addition, the inverse response of the transients [see Fig. 2(b)] also complicates the control problem. Non-minimum-phase response thus limits the amount of feedback gain that can be applied.<sup>25</sup>

To return to a mechanical example, a bicycle is an unstable system that is stabilized when moving fast enough. Assuming it is the transfer function from the steering angle of the front wheel to the tilt of the bike from the vertical has a zero in the lower-half of the complex  $\omega$  plane. If the bike is steered from the rear (with the derailleur assembly on the front wheel), the zero is in the upper-half plane. Such bicycles are almost unrideable. In 1970, Jones<sup>26</sup> described attempts to create an unrideable bicycle, using an intuitive

approach that was only partly successful (but amusing). Åström *et al.* explained how an understanding of bicycle dynamics can be used to make a truly unrideable bicycle or, more helpfully, an easier-to-ride bicycle suitable for disabled children. The authors use models of bicycle dynamics to introduce, in a very accessible way, a number of ideas about control theory.<sup>27</sup>

## VII. GENERAL IMPLICATIONS

Unlike the Kramers–Kronig relations, the Bode relation is most usefully interpreted as an inequality. If there are zeros in the upper part of the  $\omega$  plane, there will be an extra phase lag (non-minimum-phase system). In addition to producing the occasional surprise in an experiment, we saw that non-minimum-phase systems are difficult to control. Non-minimum-phase systems often correspond to situations where the input and output are separated in some way, so that there is a delay for the signal to get from the input to the output.

In the examples discussed in Sec. VI, a consistent theme was that the choice of measured variable could determine whether the response function is or is not minimum phase. Where and what is measured matters. In contrast, the resonance frequencies of a system are independent of the measurement details. In our toy example of the two-mode system, the zeros were functions of the amplitudes  $\alpha$  and  $\beta$ , but the poles that give the resonance frequencies were not. That is, the zeros of linear response functions depend on the details of the excitation and the sensor, but the poles depend on the intrinsic dynamics. The poles thus seem more fundamental than the zeros. Still, real experiments have sensors to make observations and usually actuators to create some kind of controlled excitation. Experiments always mix intrinsic dynamics with experimental details of input and output connections, and the two aspects always need to be separated. One practical lesson from the engineers is to be proactive and eliminate an upper-plane zero by rearranging sensors—choosing a different position to measure the block displacement, rotating a polarization analyzer angle, or doing more radical changes such as adding more sensors. Because the root of the problem lies in the connections of signals between the outside world and the system under study, redesigning those connections can help.

Although it might be thought that zeros and their related issues are special features of linear response, they are more general. It is true that notions of phase shifts are linked to linear systems, because they reflect a response to a sinusoidal input. In a nonlinear system, a sine-wave input generates an infinite set of harmonic sine-wave outputs, each with its own phase shift which depends on the amplitude of the input. Although there have been attempts to generalize the Kramers–Kronig (and Bode) relations to a nonlinear case, their usefulness is not clear.<sup>8</sup>

The concept of a zero is not special to linear systems. All that is required is that the output be zero for a class of input signals, so that when an output is measured, we do not know which of the input signals was responsible. For example, consider the time-domain version of an all-pass filter,

$$\dot{x}(t) = -x(t) + u(t) - \dot{u}(t). \quad (25)$$

The Fourier transform of Eq. (25) gives the response function  $G(\omega) = (1 + i\omega)/(1 - i\omega)$ , which has a non-minimum-phase zero at  $\omega = i$ . The zero here means that an input of the

form  $u(t) = u_0 e^t$  does not affect the output, no matter what the value of  $u_0$  (and even though the input diverges with time). This signal-blocking property is another important feature of zeros. Clearly, we would arrive at the same conclusion for the nonlinear equation  $\dot{x} = f(x) + u - \dot{u}$ , with  $f(x)$  a nonlinear function. Thus, there are nonlinear equations with the same pathology as linear equations. A natural formulation of the nonlinear generalization of zeros is based on geometrical tools.<sup>28</sup>

From Eq. (25), we see that the output tells us nothing about the amplitude, or even presence of the input,  $u_0$ . Such a loss of information is a familiar idea from communication theory, where the equivalent statement is that the mutual information between input and output is zero: the output gives no information about a set of inputs. The information-theory analysis of dynamical response is particularly attractive in that both nonlinear and stochastic effects can be accommodated in a natural way.<sup>29</sup>

## ACKNOWLEDGMENTS

The author is grateful for funding from NSERC (Canada) and from Simon Fraser University (for sabbatical leave). The author thanks Paul Martin, Karl Åström, Mike Plischke, Chris Homes, and Steve Dodge for their helpful suggestions. The author thanks Suckjoon Jun and Bodo Stern for making his sabbatical stay at the Harvard FAS Center for Systems Biology a pleasant and fruitful one.

## APPENDIX

We give here a brief derivation of the Kramers–Kronig relations.<sup>13–15</sup> If  $G(t)$  is a causal response function and if the response to an impulse dies away sufficiently quickly, we can assume that  $G(t) \rightarrow 0$  as  $t \rightarrow \infty$  fast enough that the integral  $\int_0^\infty G(t) e^{i\omega t} dt$  converges. If so, then the integral converges even faster for complex  $\omega$  with  $\text{Im } \omega > 0$ . As a result,  $G(\omega)$  is analytic in the complex  $\omega$ -plane for all  $\text{Im } \omega > 0$ . For simplicity, we will also assume that  $G(\omega)$  has no poles on the real axis.

Because  $G(\omega)$  is analytic for  $\text{Im } \omega \geq 0$ , we can use Cauchy’s integral theorem to write

$$\oint_{\gamma} \frac{G(\omega')}{\omega' - \omega} d\omega' = 0, \quad (A1)$$

where the closed contour  $\gamma$  is depicted in Fig. 6. The semicircular indentation around the point  $\omega$  is necessary because there is a pole in the integrand in Eq. (A1).

The integral in Eq. (A1) is divided into three parts, as labeled in Fig. 6. We have

$$\text{part I} = P \int_{-\infty}^{\infty} \frac{G(\omega')}{\omega' - \omega} d\omega', \quad (A2)$$

where  $P$  denotes the principal value, which reminds us that we have excluded an infinitesimal, symmetric region from the domain of integration.

Part II of the integral is a semicircle of radius  $r \rightarrow 0$ . We write  $\omega' = \omega + r e^{i\theta}$ , approximate  $G(\omega')$  by  $G(\omega)$ , and pull it out of the integral, leaving

$$\text{part II} = G(\omega) \int_{\pi}^0 \frac{i r e^{i\theta}}{r e^{i\theta}} d\theta = -i\pi G(\omega). \quad (A3)$$

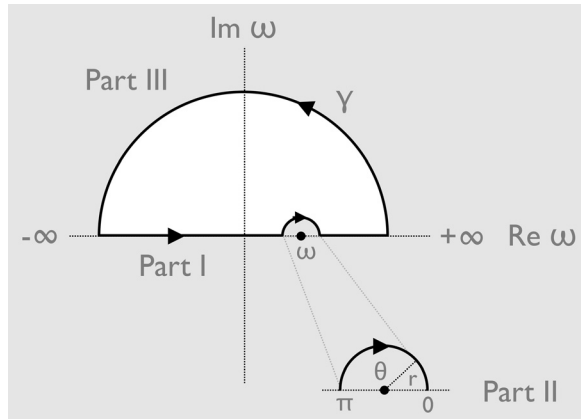


Fig. 6. Path  $\gamma$  for the contour integral in Eq. (27).

Finally, we assume that  $G(\omega') \rightarrow 0$  fast enough for  $|\omega'| \rightarrow \infty$  so that part III  $\rightarrow 0$  as the contour radius  $R \rightarrow \infty$ . Then, from the Cauchy theorem, parts I + II + III = 0, implying that

$$G(\omega) = +\frac{1}{i\pi} P \int_{-\infty}^{\infty} \frac{G(\omega')}{\omega' - \omega} d\omega'. \quad (\text{A4})$$

We write  $G = G' + iG''$  and isolate the real and imaginary to obtain gives Eq. (3).

<sup>a)</sup>Electronic mail: johnb@sfu.ca

<sup>1</sup>R. de L. Kronig, "On the theory of the dispersion of X-rays," *J. Opt. Soc. Am.* **12**, 547–557 (1926).

<sup>2</sup>H. A. Kramers, "La diffusion de la lumière par les atomes," *Atti Cong. Intern. Fisica*, (Transactions of Volta Centenary Congress) Como **2**, 545–557 (1927).

<sup>3</sup>J. S. Toll, "Causality and the dispersion relation: Logical foundations," *Phys. Rev.* **104**, 1760–1770 (1956).

<sup>4</sup>M. Shamoff, "Validity conditions for the Kramers-Kronig relations," *Am. J. Phys.* **32**, 40–44 (1964).

<sup>5</sup>H. M. Nussenzveig, *Causality and Dispersion Relations* (Academic, New York, 1972).

<sup>6</sup>F. C. Jahoda, "Fundamental absorption of barium oxide from its reflectivity spectrum," *Phys. Rev.* **107**, 1261–1265 (1957).

<sup>7</sup>D. Y. Smith, "Dispersion theory, sum rules, and their application to the analysis of optical data," in *Handbook of Optical Constants of Solids*, edited by E. D. Palik (Academic, Orlando, 1985), Vol. 2, pp. 35–68.

<sup>8</sup>K.-E. Peiponen and J. J. Saarinen, "Generalized Kramers-Kronig relations in nonlinear optical- and THz-spectroscopy," *Rep. Prog. Phys.* **72**, 056401 (2009).

<sup>9</sup>H. W. Bode, U.S. patent 2,123,178 (23, June, 1937). See H. W. Bode, "Relations between attenuation and phase in feedback amplifier design," *Bell Sys. Tech. J.* **19**, 421–454 (1940).

<sup>10</sup>H. W. Bode, *Network Analysis and Feedback Amplifier Design* (D. van Nostrand, New York, 1945).

<sup>11</sup>P. Grosse and V. Offermann, "Analysis of reflectance data using the Kramers-Kronig relations," *Appl. Phys. A* **52**, 138–144 (1991).

<sup>12</sup>D. R. Solli, C. F. McCormick, C. Ropers, J. J. Morehead, R. Y. Chiao, and J. M. Hickmann, "Demonstration of superluminal effects in an absorptionless, nonreflective system," *Phys. Rev. Lett.* **91**, 143906 (2003).

<sup>13</sup>M. Stone and P. Goldbart, *Mathematics for Physics: A Guided Tour for Graduate Students* (Cambridge U.P., Cambridge, UK, 2009).

<sup>14</sup>J. D. Jackson, *Classical Electrodynamics*, 3rd ed. (John Wiley & Sons, New York, 1999).

<sup>15</sup>W. Greiner, *Classical Electrodynamics* (Springer, New York, 1998).

<sup>16</sup>The engineering literature uses the complex  $s$  plane and Laplace transform instead of the complex  $\omega$  plane and Fourier transform. Because the two are rotated by  $90^\circ$ , our discussion of the analyticity properties in the lower and upper  $\omega$  planes is equivalent to discussions in the engineering literature of analyticity properties of the left-hand and right-hand  $s$  planes.

<sup>17</sup>In the engineering literature, Eq. (10) usually has the opposite sign. This difference traces back to the engineers' use of  $e^{-i\omega t}$  rather than  $e^{+i\omega t}$  in the forward Fourier transform.

<sup>18</sup>In formulating the gain-phase relation, we assume that the DC gain (that is, at  $\omega = 0$ ) is positive. A negative DC gain can be regarded as an overall conversion factor between input and output rather than as an extra  $180^\circ$  phase shift. Thus, for our purposes, both  $G(\omega) = -1/(1 - i\omega)$  and  $1/(1 - i\omega)$  have the same phase response.

<sup>19</sup>We also need to assume that  $G(\omega)$  has no poles in the upper half of the complex  $\omega$ -plane. Such poles correspond to unstable, exponentially growing motion and also add to the phase delay of the response. Only active systems, with external energy injection, can have such poles.

<sup>20</sup>J. C. Doyle, B. A. Francis, and A. R. Tannenbaum, *Feedback Control Theory* (MacMillan, New York, 1992), [/www.control.utoronto.ca/people/profs/francis/dft.html](http://www.control.utoronto.ca/people/profs/francis/dft.html).

<sup>21</sup>F. J. Rubio-Sierra, R. Vázquez, and R. W. Stark, "Transfer function analysis of the micro cantilever used in atomic force microscopy," *IEEE Trans. Nanotech.* **5**, 692–700 (2006). The "bad" non-minimum-phase input-output combination is to apply a distributed-force and to measure the slope at the tip. Such a situation occurs when the cantilever is excited by an external electric or magnetic field and the measurement uses the standard beam-displacement technique.

<sup>22</sup>The small imaginary part of  $\Delta n$  will shift the crossover value slightly from  $45^\circ$ .

<sup>23</sup>J. Bechhoefer, "Feedback for physicists: A tutorial essay on control," *Rev. Mod. Phys.* **77**, 783–836 (2005).

<sup>24</sup>K. J. Åström and R. M. Murray, *Feedback Systems* (Princeton U.P., Princeton, NJ, 2008).

<sup>25</sup>Another difficulty of non-minimum-phase systems is that most control loops amount to approximately inverting the transfer function of a system. Upon inversion, an upper-plane zero becomes an upper plane pole, and the inverse is unstable.

<sup>26</sup>D. E. H. Jones, "The stability of the bicycle," *Phys. Today* **59**(9), 51–56 (2006). Reprinted from *Phys. Today* **23**(4), 34–40 (1970).

<sup>27</sup>K. J. Åström, R. E. Klein, and A. Lennartsson, "Bicycle dynamics and control," *IEEE Cont. Syst. Mag.* **25**, 26–47 (2005).

<sup>28</sup>A. Isidori, *Nonlinear Control Systems*, 3rd ed. (Springer, Berlin, 1995).

<sup>29</sup>D. J. C. MacKay, *Information Theory, Inference, and Learning Algorithms* (Cambridge U.P., Cambridge, 2003).